

New High-Precision Comparison of Electron and Positron g Factors

Robert S. Van Dyck, Jr., Paul B. Schwinberg, and Hans G. Dehmelt
Department of Physics, University of Washington, Seattle, Washington 98195
 (Received 23 March 1987)

Single electrons and positrons have been alternately isolated in the same compensated Penning trap in order to form the geonium pseudoatom under nearly identical conditions. For each, the g -factor anomaly is obtained by measurement of both the spin-cyclotron difference frequency and the cyclotron frequency. A search for systematic effects uncovered a small (but common) residual shift due to the cyclotron excitation field. Extrapolation to zero power yields e^+ and e^- g factors with a smaller statistical error and a new particle-antiparticle comparison: $g(e^-)/g(e^+) = 1 + (0.5 \pm 2.1) \times 10^{-12}$.

PACS numbers: 14.60.Cd, 06.30.Lz, 12.20.Fv, 32.30.Bv

A new series of high-precision measurements of the magnetic moment (or g factor) of a single electron¹⁻³ and a single positron⁴ has been made, under nearly identical conditions (only the trapping potential is reversed) in order to produce the most exacting test of *charged* particle-antiparticle symmetry to date. The g factor (which equals twice the magnetic moment in units of Bohr magnetons) has been measured for each particle and the weighted averages of the carefully controlled runs are then compared. The new value for $g(e^-)/g(e^+)$ has been found to be consistent with unity to within ± 2 parts in 10^{12} , greatly improving upon our earlier value⁴ of $1 - (22 \pm 64) \times 10^{-12}$. The agreement between e^+ and e^- g factors can be taken as a test of *CPT* invariance to the same level of precision.

In general, a charge isolated in a Penning trap^{5,6} sees an electric restoring force along the axis of symmetry, thus producing a simple harmonic motion at ν_z which can be driven by an appropriate rf electric field. To obtain radial confinement, a strong magnetic field (≈ 50 kG) is applied along the same axis, thus generating the rapid cyclotron rotation. In addition, the axial magnetic field crossed into the antirestoring radial electric field produces a very slow magnetron drift that completes the composite cycloid motion. For e^+ and e^- , variations in respective cyclotron frequencies were less than 0.4 ppm, while differences in respective axial frequencies were less than 0.1%, and all important drive amplitudes were kept the same to within 10%.

In principle, the spin-precession frequency ν_s can be measured directly and then calibrated by use of the cyclotron frequency ν_c as a measure of the local magnetic field. In practice, since both ν_c and ν_s are nearly equal (to within 0.1%), we measure the anomaly frequency $\nu_a \equiv \nu_s - \nu_c$ and compare it to ν_c . As a result, the g -factor anomaly a , which is defined by $g = 2(1 + a)$, is given by ν_a/ν_c in free space. However, in the Penning trap environment, this simple equation is slightly modified to account for the electric shift δ_e in ν_c : $\nu_c' = \nu_c - \delta_e$, $\nu_a' = \nu_a + \delta_e$ where, under ideal conditions, this shift equals the magnetron frequency. Thus, for ei-

ther e^+ or e^- in such fields, the g -factor anomaly becomes⁷

$$a = \frac{\nu_a' - \nu_z^2/2\nu_c'}{\nu_c' + \nu_z^2/2\nu_c'}$$

where δ_e is replaced by its value obtained from the equation of motion.

The basic apparatus is a compensated Penning trap⁸ with special guard rings and hyperbolic end caps and ring electrodes which coincide with quadratic equipotentials. As before,^{3,4} electrons are obtained from a field-emission point located in one of the end caps, whereas positrons, moderated from a ²²Na source, are trapped via radiation damping in a specially designed storage trap.⁹ Subsequently, some positrons are pulsed into the experiment trap where on one occasion, a single e^+ was kept continuously trapped for 111 days, while we used it for several $g - 2$ runs.

The special guard electrodes are split on one side only in order to effectively generate a set of countercirculating current loops.³ A tuned rf transformer applies the same current to both loops, thus generating a linearly increasing radial rf magnetic field at ν_a' . This feature is an important improvement over our previous trap^{1,3,4,10} which used a static magnetic bottle and a very strong electric axial drive at ν_a' to produce the required radial magnetic field at the precession frequency.

The primary function of the magnetic bottle (through its second-order gradient) is to couple the total magnetic moment of the charge to the very precise harmonic frequency ν_z (whose resolution exceeds 10 ppb). The effect of this coupling is a frequency dependence of the form $\nu_z \approx \nu_{z0} + (n + m + \frac{1}{2})\delta$ where n and m are cyclotron and spin-precession quantum numbers, respectively, and $\delta = 1.3 \pm 0.2$ Hz for the bottle in question (see Fig. 1). By incorporation of the driven axial response into a feedback loop, a ring-electrode correction voltage¹⁰ has been obtained which reflects the sum of quantum numbers $n + m + \frac{1}{2}$. A more complete description of the frequency-shift detection method^{1,10} (or continuous Stern-

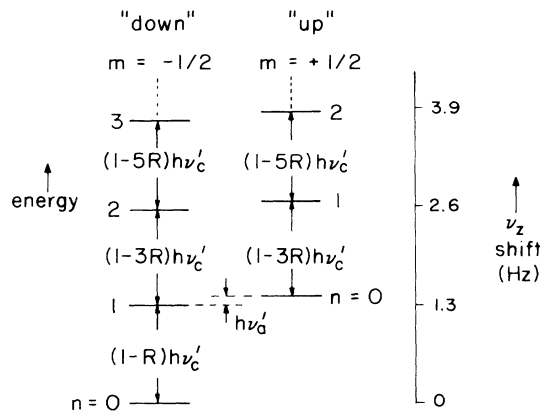


FIG. 1. Simplified energy-level diagram for geonium. The axial frequency shift (shown in the right-hand scale as 1.3 Hz/level) corresponds to the coupling via the axial magnetic bottle field. The $h\nu'_a$ energy difference and relativistic shift ($R=0.5$ ppb) have been exaggerated for clarity; vanishing axial and magnetron energies are also assumed.

Gerlach effect^{1,11,12}) is given elsewhere. An additional feature of this magnetic bottle is that magnetic resonances will exhibit a $z=0$ low-frequency edge and a high-frequency tail which reflects the average axial thermal energy^{1,2,10} through $\langle z^2 \rangle_{av}$, similar to that shown in the anomaly resonance (see Fig. 2).

One of the major improvements in technique has been the use of an "assist" in cyclotron-state excitation during the ν'_a measurement. In theory, an e^+ or e^- would spend $\approx 80\%$ of its time in the lowest ($n=0$) cyclotron quantum state (see Fig. 1), under the assumption that the ambient temperature is 4 K. In the lowest spin-down state, the ν'_a field cannot induce spin flips. However, in the spin-up state, a two-photon transition can always couple the lowest levels. Therefore, to increase the temperature of the cyclotron motion effectively and thus to enhance the flipping rate from "down" to "up", the ν'_c excitation power is also applied during the ν'_a excitation, except that the microwave frequency is shifted 5–10 kHz into the tail of the cyclotron resonance in order to mimic a random-phase thermal excitation. As a result, much *less* anomaly power is required to obtain the same number of spin flips and the *same* microwave power can be kept on during both ν'_a and ν'_c measurements. To complete the symmetry, anomaly power remains on when ν'_c is determined, but shifted several kilohertz away from the ν'_a resonance.

Finally, a small shift in trapping potential is produced during the ν'_c , ν'_a excitation phases in order to reduce axial damping. A Brownian-motion line-shape theory¹³ has confirmed that the anomaly resonance will have a sharper¹¹ $z=0$ edge if the axial linewidth is reduced well below the magnetic resonance width. This axial damping width is inversely proportional to $1 + (\epsilon/\Delta\nu)^2$, where

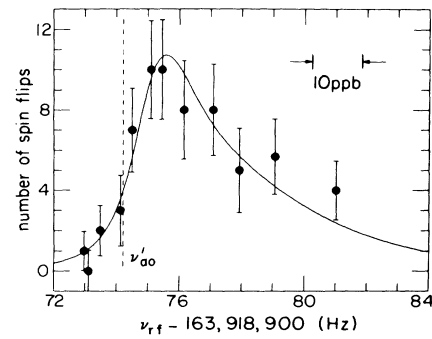


FIG. 2. Single-electron (geonium) anomaly resonance. Each point represents 25 measurements of the spin state. The line shape shows the characteristic exponential tail, but with a low-frequency edge which is not as sharp as normally found in ν'_c resonances. A sharp vertical edge (Ref. 11) at ν'_{a0} would be observable only in the limit of no axial damping. Error bars are derived from the binomial distribution, and are computed with the least-squares-fitted curve as the true parent distribution. A typical fitted $z=0$ edge is uncertain by 0.2 Hz.

ϵ is the detuning of the axial frequency relative to the (detection) tuned-circuit resonance whose half-width at half maximum is $\Delta\nu$. In both cases, the *natural* width of each magnetic resonance is given by $1/2\pi\tau_c$ where τ_c is the factor-of-10 inhibited damping time, measured³ to be ≈ 1 sec. A corresponding improvement in the analysis comes from fitting of data by the theoretical line shape¹³ and thus determining the $z=0$ anomaly edge to a precision of ≈ 1 ppb (see Fig. 2).

The simultaneous application of constant-amplitude magnetic drives has greatly reduced previously observed systematic power shifts. However, a residual shift, common to e^+ and e^- , still exists due to the measurement process of sweeping up-frequency toward the cyclotron edge. For excitation to $n > 1$, a relativistic shift to a lower frequency is expected (see Fig. 1). A more complete line-shape theory which incorporates the relativistic shift could presumably account for this observed power shift. Finite width of the microwave source, or remaining X-band radiation leaking into the trap, may be contributing factors. The strong X-band field (at 8.8 GHz) is required to generate a harmonic at 141 GHz. Figure 3 shows the residual shift of the ν'_c -resonance edge versus the applied microwave power which is related to the rectified current through the multiplier diode according to ≈ 0.0175 dB/ μ A.

Table I summarizes the results of the nine runs on both single electrons and single positrons, taken with some similar variations of microwave power and rf anomaly power. The latter is measured as a shift in the axial frequency due to an additional trapping field, consistent with the theory of rf or Paul traps.^{6,14} The last column shows the anomaly corrected for the systematic shift in measured cyclotron frequency, relative to 310

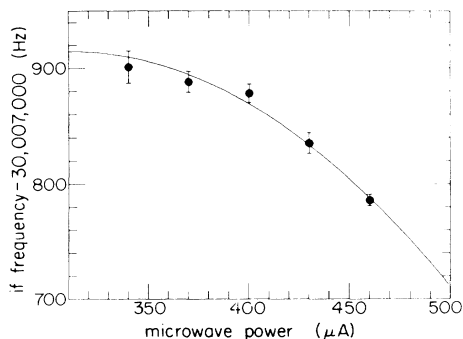


FIG. 3. Residual systematic shift of $\nu'_c(e^-)$ versus applied X-band microwave power. The vertical scale denotes the intermediate frequency where $\nu'_c = 16[\nu_{\text{rf}} + 8803699296 \text{ Hz}]$ and the horizontal scale is in units of rectified X-band current in the multiplier diode. The solid curve represents a quadratic fit to these data with the constraint that the "zero" for the sixteenth harmonic be fixed at $310 \mu\text{A}$.

μA —the approximate zero for the 141-GHz microwave field (at which point the $n=1$ level is not appreciably excited). Note that all the values agree within statistical errors. Thus, in the limit of zero microwave power, the electron anomaly is given as

$$a(e^-) = 1159652188.4(4.3) \times 10^{-12}.$$

The error quoted reflects the statistical uncertainty of 0.62×10^{-12} in the weighted average, an estimate of residual microwave power shift of 1.3×10^{-12} , and our estimate¹⁵ of 4×10^{-12} for the shift associated with cavity effects. This result can be compared to our previous value,³ $1159652193(4) \times 10^{-12}$, where the large ob-

TABLE I. Summary of e^+ and e^- runs taken under very similar conditions with variations in anomaly (rf) and cyclotron (microwave) drives as shown, and all cyclotron calibrations made relative to "spin-down" state. The fourth column shows a correction for systematic dependence on microwave power and corrected anomalies have statistical errors included.

| Charge | rf power ^a (Hz) | Microwave power ^b (μA) | Relative a_e shift (ppb) | [(Corrected a_e) - 1159652000] $\times 10^{-12}$ |
|--------|-------------------------------|---------------------------------------------------|-------------------------------|-----------------------------------------------------------|
| e^+ | 300 | 380 | -3.14 | 186.80(2.73) |
| e^+ | 310 | 366 | -2.01 | 184.88(2.49) |
| e^+ | 390 | 372 | -2.46 | 188.49(1.86) |
| e^+ | 470 | 371 | -2.38 | 186.91(1.93) |
| e^+ | 470 | 380 | -3.14 | 190.28(1.83) |
| e^- | 480 | 370 | -2.30 | 188.95(1.31) |
| e^- | 500 | 320 | -0.06 | 188.67(1.49) |
| e^- | 400 | 330 | -0.26 | 188.20(1.14) |
| e^- | 500 | 350 | -1.02 | 188.09(1.12) |

^aUnits measured as shift in ν_c .

^bUnits measured as current through diode.

served scatter in those previous runs may have been due to the same systematic shift of the ν'_c edge versus the (then unlevelled) microwave power.

Clearly, the largest uncertainty is associated with a possible shift^{11,16} of ν'_c due to close proximity of possible microwave-cavity resonances. Recently, we have developed a method for observing these modes and now conclude that the trap has a cavity $Q \leq 500$. Combining this with the restraint that the cyclotron damping is inhibited by a factor of 10, we estimate,¹⁷ for the relative shift in ν'_a , a worst-case error consistent with the above conditions of 4 ppb.

Similarly, the positron runs are corrected for the known shift in ν'_c due to finite 141-GHz microwave power:

$$a(e^+) = 1159652187.9(4.3) \times 10^{-12},$$

where the errors have the same meaning as given above. Positron runs generally appear to have a larger statistical error whose causes are not yet well understood. This single-positron anomaly can also be compared to our previous result,⁴ $115965222(50) \times 10^{-12}$, where the large uncertainty in that case was due to the incorrect assignment of the ν'_a edge before line-shape fitting became available. Upon comparing our new results, we obtain

$$g(e^-)/g(e^+) = 1 + (0.5 \pm 2.1) \times 10^{-12},$$

which represents the most accurate demonstration of charged particle-antiparticle symmetry known to date, exceeded only by a high-energy comparison of a different nature on the neutral $K-\bar{K}$ system.¹⁸

Probably the most satisfying accomplishment of this work is its agreement with theory. Using quantum electrodynamics, Kinoshita has calculated the $(\alpha/\pi)^4$ term in the anomaly in order to produce a preliminary determination¹⁹ of $a_e = 1159652263(22)(104) \times 10^{-12}$ with further improvement in progress. The first error is due to the calculation and the second is contributed by the uncertainty in the fine-structure constant²⁰: $\alpha^{-1} = 137.0359815(123)$. However, by combination of theory and our experiment, a new QED fine-structure constant can be determined: $\alpha^{-1} = 137.0359900(27)$ where the ≈ 5 times smaller uncertainty is dominated by the error in the theoretical calculation. This result disagrees somewhat with the most recent α^{-1} values of 137.0360120(110) based on the quantized Hall effect²¹ and 137.0360302(76) if a recent calculation²² by Samuel is employed.

An important future improvement in the apparatus will involve the use of a variable superconducting magnetic bottle²³ which can be used with ac methods²⁴ to increase signal-to-noise ratio, and, in a dc fashion, to compensate for any intrinsic bottle magnetic field,²⁵ and also to stabilize²³ the main magnetic field further. In addition, the next trap will feature a very low cavity Q to reduce^{16,17} any possible shift in ν'_c and thus ν'_a .

We are indebted to Lowell Brown for his intricate analysis of the anomaly resonance's line shape and to Fred Moore for his meticulous efforts at generating the reliable FORTRAN code used for least-squares fitting. In addition, we are pleased to thank the instrument makers who machined the high-precision trapping electrodes. This work is supported by the National Science Foundation under the "Single Elementary Particle at Rest in Free Space" project.

¹For a description of earlier precision measurements on a single electron, see R. S. Van Dyck, Jr., P. B. Schwinberg, and H. G. Dehmelt, *Phys. Rev. D* **34**, 722 (1986).

²A review of geonium theory can be found in L. S. Brown and G. Gabrielse, *Rev. Mod. Phys.* **58**, 233 (1986).

³R. S. Van Dyck, Jr., P. B. Schwinberg, and H. G. Dehmelt, in *Atomic Physics 9*, edited by R. S. Van Dyck, Jr., and E. N. Fortson (World Scientific, Singapore, 1984), p. 53.

⁴P. B. Schwinberg, R. S. Van Dyck, Jr., and H. G. Dehmelt, *Phys. Rev. Lett.* **47**, 1679 (1981).

⁵F. M. Penning, *Physica (Utrecht)* **3**, 873 (1936).

⁶Penning traps are also reviewed by H. G. Dehmelt in *Adv. At. Mol. Phys.* **3**, 53 (1967).

⁷Even in a not-so-ideal environment, the simple modification as described still applies to a high degree: L. Brown and G. Gabrielse, *Phys. Rev. A* **25**, 2423 (1982), and Ref. 1.

⁸R. S. Van Dyck, Jr., D. J. Wineland, P. A. Ekstrom, and H. G. Dehmelt, *Appl. Phys. Lett.* **28**, 446 (1976).

⁹This first antimatter trapping was accomplished in 1979; see P. B. Schwinberg, R. S. Van Dyck, Jr., and H. G. Dehmelt, *Phys. Lett.* **81A**, 119 (1981).

¹⁰R. Van Dyck, Jr., P. Schwinberg, and H. Dehmelt, in *New*

Frontiers in High Energy Physics, edited by B. Kursunoglu, A. Perlmutter, and L. Scott (Plenum, New York, 1978), p. 159.

¹¹H. Dehmelt, in *Atomic Physics 7*, edited by D. Kleppner and F. Pipkin (Plenum, New York, 1981), p. 337.

¹²H. Dehmelt, *Proc. Natl. Acad. Sci. U.S.A.* **83**, 2291 (1986).

¹³L. S. Brown, *Phys. Rev. Lett.* **52**, 2013 (1984), and *Ann. Phys. A* **159**, 62 (1985).

¹⁴E. Fischer, *Z. Phys.* **156**, 1 (1959).

¹⁵Estimates based on cylindrical-cavity model found in L. Brown, G. Gabrielse, K. Helmerson, and J. Tan, *Phys. Rev. A* **32**, 3204 (1985), have confirmed earlier estimates [H. Dehmelt, *Proc. Natl. Acad. Sci. U.S.A.* **81**, 8037 (1984), and **82**, 6366 (1985)].

¹⁶Dehmelt, Ref. 15.

¹⁷H. Dehmelt, R. Van Dyck, Jr., G. Gabrielse, P. Schwinberg, *et al.*, unpublished.

¹⁸C. G. Wohl *et al.* (Particle Data Group), *Rev. Mod. Phys.* **56**, S1 (1984).

¹⁹T. Kinoshita, in *Proceedings of the Conference on Precision of Electromagnetic Measurements*, Gaithersburg, Maryland, 1986, to be published.

²⁰B. N. Taylor, *J. Res. Natl. Bur. Stand.* **90**, 91 (1985), and private communication.

²¹G. Sloggett, K. Clothier, and B. Ricketts, *Rev. Lett.* **57**, 3237 (1986).

²²M. Samuel, *Phys. Rev. Lett.* **57**, 3133 (1986).

²³R. S. Van Dyck, Jr., F. L. Moore, D. L. Farnham, and P. B. Schwinberg, *Rev. Sci. Instrum.* **57**, 593 (1986).

²⁴P. B. Schwinberg and R. S. Van Dyck, Jr., *Bull. Am. Phys. Soc.* **26**, 598 (1981).

²⁵G. Gabrielse and H. Dehmelt, *Bull. Am. Phys. Soc.* **26**, 598 (1981).